



# Establishment and characterization of CRISPR/Cas9-mediated *NF2*<sup>-/-</sup> human mesothelial cell line: Molecular insight into fibroblast growth factor receptor 2 in malignant pleural mesothelioma

Md Wahiduzzaman<sup>1</sup> | Sivasundaram Karnan<sup>1</sup>  | Akinobu Ota<sup>1</sup>  | Ichiro Hanamura<sup>2</sup> | Hideki Murakami<sup>3</sup> | Akihito Inoko<sup>4</sup> | Md Lutfur Rahman<sup>1</sup> | Toshinori Hyodo<sup>1</sup> | Hiroyuki Konishi<sup>1</sup> | Shinobu Tsuzuki<sup>1</sup> | Yoshitaka Hosokawa<sup>1</sup>

<sup>1</sup>Department of Biochemistry, Aichi Medical University School of Medicine, Nagakute, Japan

<sup>2</sup>Division of Hematology, Department of Internal Medicine, Aichi Medical University School of Medicine, Nagakute, Japan

<sup>3</sup>Department of Pathology, Aichi Medical University School of Medicine, Nagakute, Japan

<sup>4</sup>Division of Cancer Epidemiology and Prevention, Aichi Cancer Center Research Institute, Nagoya, Japan

## Correspondence

Sivasundaram Karnan, Department of Biochemistry, Aichi Medical University School of Medicine, Nagakute, Japan.  
Email: skarnan@aichi-med-u.ac.jp

## Funding information

Hirose International Scholarship Foundation

Malignant pleural mesothelioma (MPM), a highly refractory tumor, is currently incurable due to the lack of an early diagnosis method and medication, both of which are urgently needed to improve the survival and/or quality of life of patients. *NF2* is a tumor suppressor gene and is frequently mutated in MPM. Using a CRISPR/Cas9 system, we generated an *NF2*-knockout human mesothelial cell line, MeT-5A (*NF2*-KO). In *NF2*-KO cell clones, cell growth, clonogenic activity, migration activity, and invasion activity significantly increased compared with those in *NF2*-WT cell clones. Complementary DNA microarray analysis clearly revealed the differences in global gene expression profile between *NF2*-WT and *NF2*-KO cell clones. Quantitative PCR analysis and western blot analysis showed that the upregulation of fibroblast growth factor receptor 2 (*FGFR2*) was concomitant with the increases in phosphorylation levels of JNK, c-Jun, and retinoblastoma (Rb) in *NF2*-KO cell clones. These increases were all abrogated by the exogenous expression of *NF2* in the *NF2*-KO clone. In addition, the disruption of *FGFR2* in the *NF2*-KO cell clone suppressed cell proliferation as well as the phosphorylation levels of JNK, c-Jun, and Rb. Notably, *FGFR2* was found to be highly expressed in *NF2*-negative human mesothelioma tissues (11/12 cases, 91.7%) but less expressed in *NF2*-positive tissues. Collectively, these findings suggest that *NF2* deficiency might play a role in the tumorigenesis of human mesothelium through mediating *FGFR2* expression; *FGFR2* would be a candidate molecule to develop therapeutic and diagnostic strategies for targeting MPM with *NF2* loss.

## KEYWORDS

CRISPR/Cas9, *FGFR2*, mesothelioma, microarray, *NF2*

**Abbreviations:** BAP1, BRCA1-associated protein-1; Cas9, CRISPR-associated protein 9; CDK2, cyclin-dependent kinase 2; CDKN2A, cyclin-dependent kinase inhibitor 2A; CRISPR, clustered regularly interspaced short palindromic repeats; *FGFR2*, fibroblast growth factor receptor 2; MPM, malignant pleural mesothelioma; *NF2*, neurofibromatosis type 2; qRT-PCR, quantitative real-time PCR; Rb, retinoblastoma; sgRNA, single guide RNA; sh, short hairpin; YAP, yes-associated protein.

This is an open access article under the terms of the Creative Commons Attribution-NonCommercial License, which permits use, distribution and reproduction in any medium, provided the original work is properly cited and is not used for commercial purposes.

© 2018 The Authors. *Cancer Science* published by John Wiley & Sons Australia, Ltd on behalf of Japanese Cancer Association.

## 1 | INTRODUCTION

Malignant pleural mesothelioma, an aggressive neoplasm that arises from pleural mesothelial cells, is associated with asbestos exposure after 20-40 years of latency.<sup>1,2</sup> Patients with MPM are usually diagnosed at an advanced stage of the disease, and their prognosis remains poor. Median survival after diagnosis is 6-12 months, and the standard-of-care agents, pemetrexed and cisplatin, are relatively ineffective at increasing the survival time.<sup>3,4</sup> Asbestos could have multiple effects in carcinogenesis, but the molecular mechanisms underlying asbestos-induced tumorigenesis are still unclear.<sup>5,6</sup>

Recent molecular biological studies have revealed frequent genetic alterations in patients with MPM, with 3 key tumor suppressor genes, *NF2*, *CDKN2A*, and *BAP1*, being identified at rates of 30%-50%, 70%, and 20%-60% in MPM cases, respectively.<sup>7-13</sup> Moreover, the status of these 3 genes has significant prognostic implications. Homozygous *CDKN2A* deletions are a poor prognostic indicator for patients with MPM.<sup>14-16</sup> Deletion of *NF2* is associated with increased cell proliferation, invasiveness, spreading, and migration.<sup>17,18</sup> However, the molecular mechanism by which normal mesothelial cells acquire a carcinogenic phenotype in humans is not well understood. In this study, we first examined the effect of *NF2* loss on the gene expression profile in human normal mesothelium cell line MeT-5A and then characterized the cellular phenotype *in vitro*. We focused on one of the *NF2*-related genes, *FGFR2*, and showed the involvement of *FGFR2* in the cellular phenotype in *NF2*-KO cell clones. We also investigated the association between *NF2* loss and *FGFR2* expression in MPM tissues.

## 2 | MATERIALS AND METHODS

### 2.1 | Cell culture

Three immortalized normal human mesothelial cell lines, MeT-5A (pleural mesothelial), HOMC-A4 (omental mesothelial; sarcomatoid type), and HOMC-D4 (omental mesothelial; intermediate type), and 1 human mesothelioma cell line, NCI-H2052, were kindly provided by Dr. Y. Sekido, Division of Molecular Oncology, Aichi Cancer Center Research Institute (Nagoya, Japan). HOMC-A4 and HOMC-D4 cell lines were maintained as described elsewhere.<sup>19</sup> MeT-5A and NCI-H2052 cell lines were maintained in RPMI-1640 (Wako, Osaka, Japan) medium containing 10% FBS (Sigma-Aldrich St. Louis, MO, USA) and penicillin-streptomycin (Wako) at 37°C in a 5% CO<sub>2</sub> air atmosphere.

### 2.2 | Gene knockout using the CRISPR/Cas9 system

The CRISPR/Cas9 system was used to disrupt the expression of the *NF2* and *FGFR2* genes, as described elsewhere.<sup>20</sup> pSpCas9(BB)-2A-GFP (PX458) was a gift from Feng Zhang (plasmid #48138; Addgene, Watertown, MA, USA).<sup>20</sup> In brief, an sgRNA sequence was selected using an Optimized CRISPR Design (<http://crispr.mit.edu/>). The sgRNA sequence for *NF2* was 5'-AAACATCTCGTACAGTGACA-3'

and that for *FGFR2* was 5'-GTACCGTAACCATGGTCAGC-3', corresponding to exons 8 and 1, respectively. The plasmid expressing hCas9 and the sgRNA was prepared by ligating oligonucleotides into the *BbsI* site of PX458 (*NF2*/PX458 and *FGFR2*/PX458). To establish a knockout clone, 1 µg *NF2*/PX458 or *FGFR2*/PX458 plasmid was nucleofected into cells (1 × 10<sup>6</sup> cells) using a 4D-Nucleofector instrument (Lonza Japan, Tokyo, Japan). After 3 days, the cells expressing GFP were sorted using FACS (BD Biosciences, San Jose, CA, USA). A single clone was selected, expanded, and then used for biological assays. For sequence analysis of the *NF2* gene, the following primer set was used: forward, 5'-CAGTTTTGCTTCTACCTGCC-3' and reverse, 5'-GCCAGTTGAGCTTCCCAGTT-3'.

### 2.3 | Construction of RNAi vectors and expression vectors

To construct an RNAi vector, sh oligonucleotide was inserted into pLentiLox3.7 plasmid (Addgene) under the control of the U6 promoter. Two sh oligonucleotides were designed for the target sequence of the hairpin loop of YAP (sh1, 5'-TTCTATGTTTCATCCATCTCC-3'; sh2, 5'-GAGTTCTGACATCCTTAAT-3'). A control shRNA vector was also constructed using a scrambled sequence for YAP (scr1, 5'-GGATAAACTAAGGGATAGGAA-3'). To construct the expression vector, cDNA fragments of WT YAP and *NF2* were amplified by PCR using Prime STAR Max DNA polymerase (Takara Bio, Otsu, Japan). The phosphorylation-defective mutant YAP (YAP<sup>S127/381A</sup>) was constructed by *in vitro* mutagenesis at codons 127 and 381 from serine to alanine (S127/381A). The cDNA fragments were then introduced into the pcDNA3.1 expression vector (Addgene). Backbone pcDNA3.1 was used as a control vector. The cells (1 × 10<sup>6</sup> cells) were nucleofected with 1 µg of each vector using a 4D-Nucleofector instrument (Lonza Japan).

### 2.4 | Quantitative real-time PCR

Quantitative real-time PCR analysis was carried out using SYBR Green I, as previously described.<sup>21</sup> *GAPDH* was used as an internal control. The primers used in this study are described in Table S1.

### 2.5 | Complementary DNA microarray analysis

The experimental procedure for the cDNA microarray analysis was based on the manufacturer's protocol (Agilent Technologies, Santa Clara, CA, USA). In brief, cDNA synthesis and cRNA labeling with the cyanine 3 dye were carried out using the Agilent Low Input Quick Amp Labeling Kit (Agilent Technologies). The cyanine 3-labeled cRNA was purified, fragmented, and hybridized on a Human Gene Expression 4 × 44K v2 Microarray Chip containing 27 958 Entrez Gene RNAs, using a Gene Expression Hybridization kit (Agilent Technologies). The raw and normalized microarray data have been submitted to the GEO database at NCBI (accession no. GSE116000; <https://www.ncbi.nlm.nih.gov/geo/query/acc.cgi?acc=GSE116000>). Gene set enrichment analysis was carried out according to the instructions.

## 2.6 | Cell growth assay

The cell growth rate was determined by an MTT assay. Briefly, the cells ( $1 \times 10^3$  cells/well) were seeded into a 96-well plate and cultured for indicated times. Subsequently, 10  $\mu$ L MTT solution (5 mg/mL; Sigma-Aldrich) was added to each well, and the cells were further incubated for 4 hours. Next, the cell lysis buffer was added to the wells to dissolve the colored formazan crystals produced by MTT. The absorbance at 595 nm was measured using a SpectraMAX M5 spectrophotometer (Molecular Devices, Sunnyvale, CA, USA).

## 2.7 | Soft agar colony formation assay

The soft agar colony formation assay was carried out as described previously.<sup>22</sup> The number of colonies was counted using Colony Counter software (Keyence, Tokyo, Japan). The data are presented as mean  $\pm$  SEM ( $n = 3$ ).

## 2.8 | Wound healing assay and migration assay

The cells were cultured as a monolayer in 12-well plates. Upon reaching approximately 60%-70% confluence, wounds were made by scratching using pipette tips. After washing with PBS, the wounds were photographed every 24 hours. Ten thousand cells suspended in 100  $\mu$ L serum-free medium were added into the upper chambers of a Transwell (8  $\mu$ m for 24-well plate; Millipore, Tokyo, Japan), and culture medium was added into the lower chambers. After 24 hours, the cells were fixed by formalin and stained by 0.1% crystal violet. The number of colonies was manually counted under a microscope.

## 2.9 | Western blot analysis

Western blot analysis was carried out as described previously.<sup>22</sup> The antibodies used in this study are described in Table S2. Immune

complexes were detected using ImmunoStar LD (Wako) in conjunction with a LAS-4000 image analyzer (GE Healthcare, Tokyo, Japan).

## 2.10 | Immunohistochemistry

Immunohistochemical analysis was carried out according to the procedure previously described.<sup>23</sup> The human mesothelioma tissue array was purchased from US Biomax (MS-801a; Rockville, MD, USA). The sections were reacted with a primary Ab (anti-FGFR2 or anti-NF2 Ab, 2  $\mu$ g/mL). Normal rabbit IgG or omission of primary Abs served as negative controls. Immunoreactivity was evaluated independently by 2 investigators (S.K. and H.M.). The intensity of staining was scored as strong (3+), moderate (2+), weak (1+), or negative (0).

## 2.11 | Statistical analysis

Results are expressed as mean  $\pm$  SE. Statistical significance between groups was determined using one-way ANOVA and Dunnett's comparison. Statistical analyses were undertaken using SPSS 23.0 program (SPSS, Chicago, IL, USA).

## 3 | RESULTS

### 3.1 | Loss of NF2 enhances cell proliferation, colony formation, and migration in MeT-5A cells

To investigate the role of NF2 in the survival and proliferation of MPM cells, we established NF2-knockout cell clones (hereafter called NF2-KO #1 and #2) in a human mesothelial cell line, MeT-5A, by using a CRISPR/Cas9 system targeting exon 8 of the NF2 gene. DNA sequencing analysis showed that the NF2-KO cell clones possessed frameshift mutations, which harbored either 200-bp (NF2-KO #1) or 22-bp (NF2-KO #2) deletions in the NF2 gene (Figure 1A). We also randomly selected two MeT5A/NF2<sup>+/+</sup> cell clones (hereafter called NF2-WT #1 and #2), which had not been targeted by the Cas9

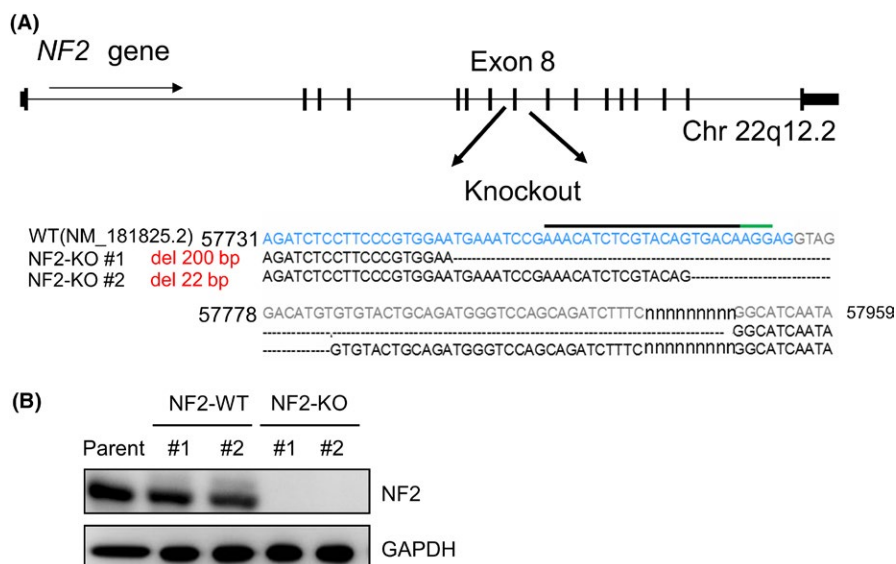


**FIGURE 1** Generation of neurofibromatosis type 2 (NF2) knockout (NF2-KO) cell clones using a CRISPR/Cas9 system with the human mesothelial cell line MeT-5A. A, A single guide RNA sequence was designed against exon 8 of the NF2 locus. Sequences of the parental and NF2-KO cell clones #1 (200-bp deletion) and #2 (22-bp deletion) were analyzed, and the results are shown below. The single guide RNA sequence and the protospacer adjacent motif (PAM) sequence are indicated by a black and green overline, respectively. The exon 8 sequence of NF2 is described in blue letters. B, NF2 protein expression was determined by western blot analysis. GAPDH was used as an internal control

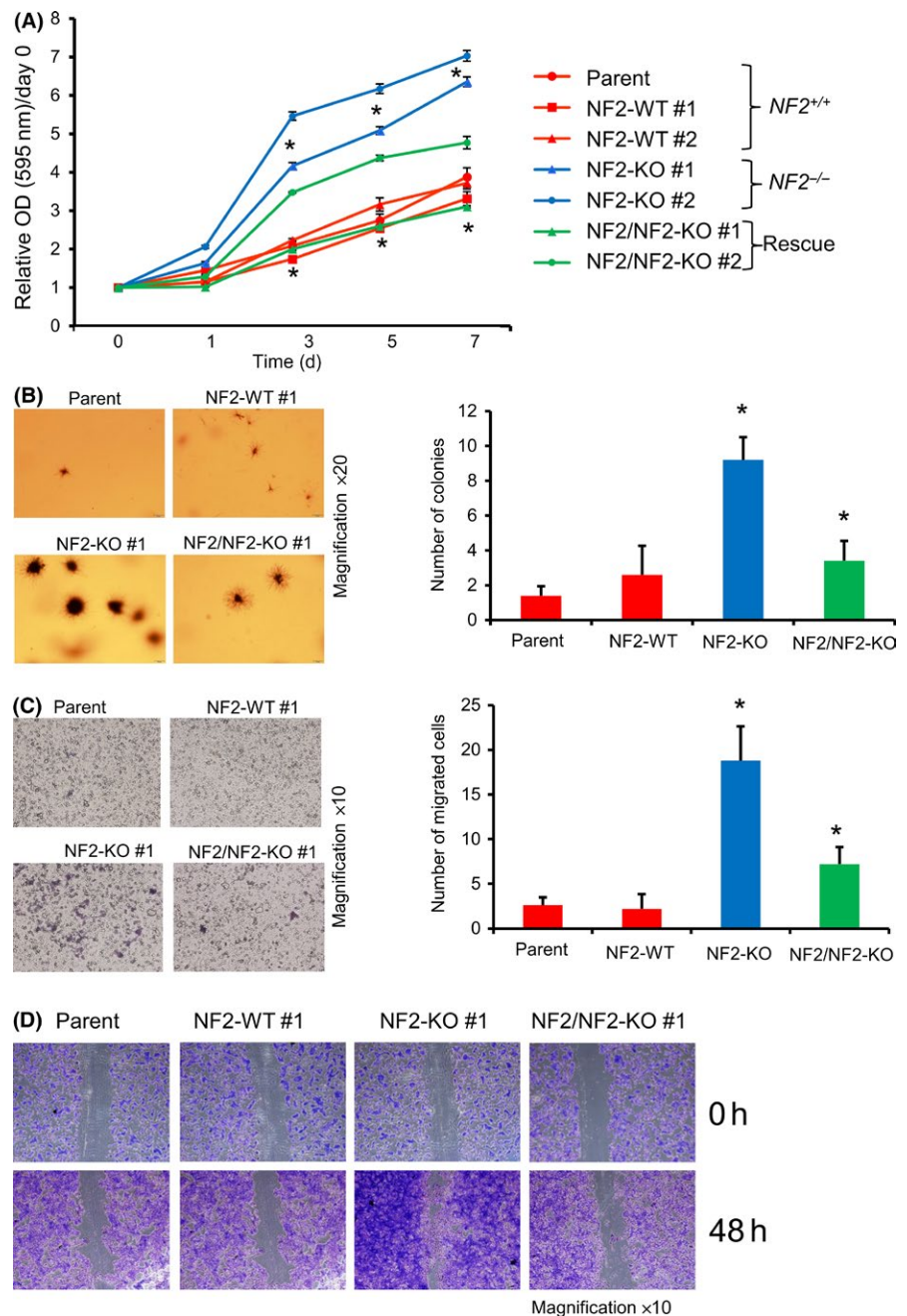
vector. Western blot analysis detected no protein expression of NF2 in the NF2-KO clones, but solid NF2 expression in the parental cells and NF2-WT clones (Figure 1B). Using these established clones, we first examined the cell proliferation using the MTT assay, and found that the cell growth ratio was significantly increased in the NF2-KO clones, compared with that in the parental cells and NF2-WT clones (Figure 2A). In addition, NF2-KO clone formed more colonies in soft agar, compared with NF2-WT clones and parent (Figure 2B). Furthermore, migration and wound-healing activities were significantly higher in the NF2-KO clone (Figure 2C,D). To further confirm the effect of NF2 on the tumorigenic properties of the NF2-KO cells, we generated the cells exogenously expressing NF2 in the NF2-KO clone (hereafter called NF2/NF2-KO #1 and #2). We found that

rescuing NF2 in the NF2-KO cells significantly suppressed the cell proliferation, colony formation, migration, and wound-healing activities induced by NF2 mutation (Figure 2). These results suggest that NF2 inactivation enhances the proliferation, clonogenicity, and migration of normal mesothelial cells. Similar to our results, the significance of NF2 mutation in the proliferation, clonogenicity, and migration of MPM cells has been reported elsewhere.<sup>17,18,24,25</sup>

### 3.2 | Global gene expression change induced by disruption of NF2

To identify the genes related to enhanced proliferation in the NF2-KO clones, we undertook comprehensive cDNA microarray analyses in

**FIGURE 2** Cellular phenotype of neurofibromatosis type 2 knockout (NF2-KO) MeT-5A cells. A, MTT analysis of the growth rate of parental MeT-5A cells, control NF2-WT cell clones (#1 and #2), NF2-KO cell clones (#1 and #2), and NF2/NF2-KO cell clones (#1 and #2). The relative optical density (OD) at 595 nm was calculated by dividing the OD of day 0 at each time point (days 0, 1, 3, 5, and 7) and is presented as the mean  $\pm$  SEM ( $n = 3$ ). B, Representative soft agar colony formation assay. Two hundred cells of each clone were seeded in a 6-well plate. After 14 days, the cells were stained with MTT and imaged. Right bar graphs represent the number of stained colonies. Data are presented as the mean  $\pm$  SEM ( $n = 3$ ). C, Representative migration assay with a Boyden chamber. Cells were seeded in a Boyden chamber on a 24-well plate ( $2.5 \times 10^5$  cells/well). After 24 hours, the cells were stained with crystal violet and imaged. Right bar graph represents the number of stained colonies. Data are presented as the mean  $\pm$  SEM ( $n = 3$ ). D, Representative scratch assay. Each cell clone was seeded in a 24-well plate ( $1 \times 10^5$  cells/well) and incubated at 37°C. When the cell density reached ~60%-70% confluence, the cells were gently scratched with a new 1-mL pipette tip across the center of the well. After scratching, the cells were incubated for 48 hours and then stained with crystal violet and imaged. \*Statistically significant difference ( $P < .05$ )



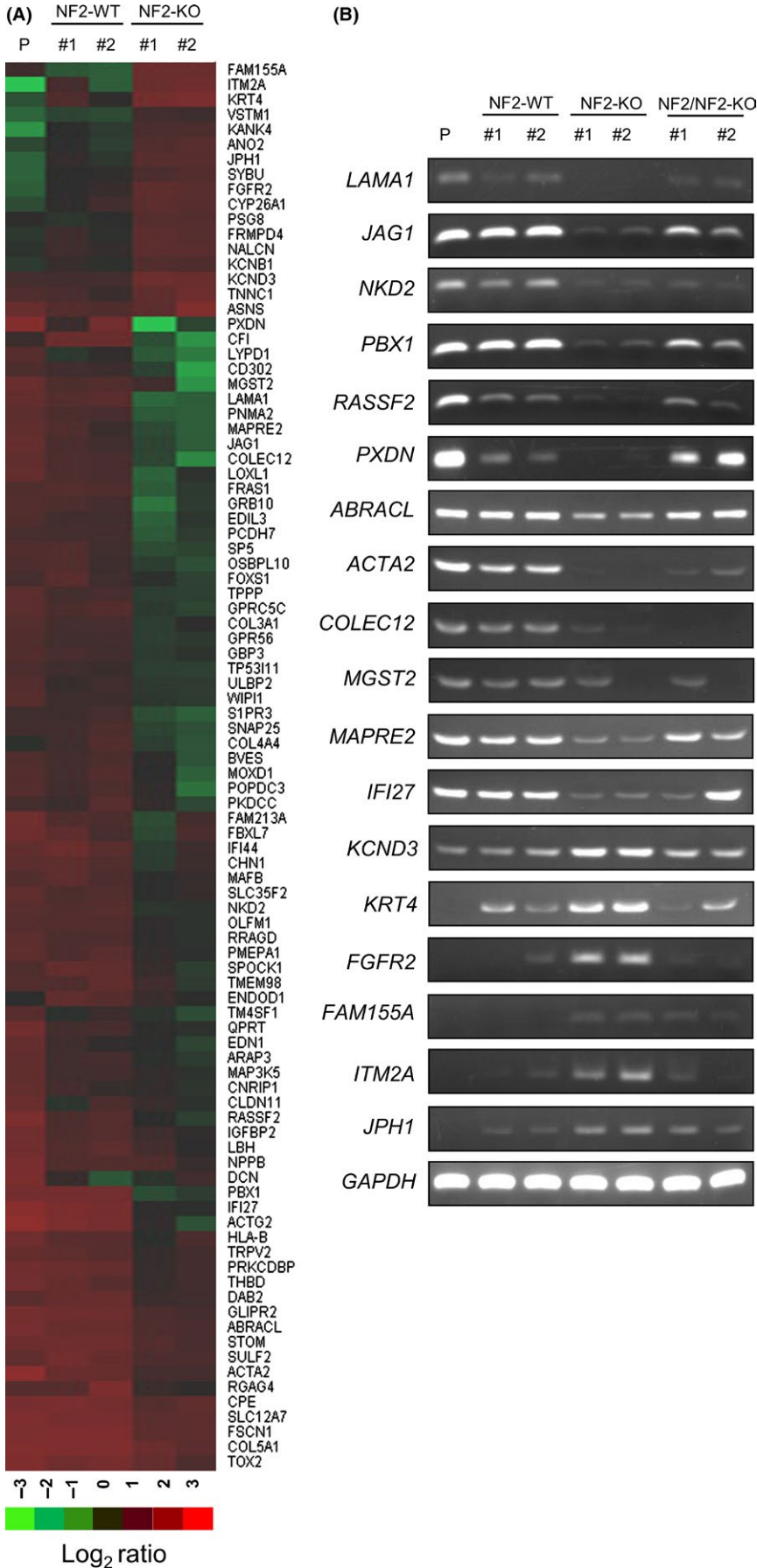


**FIGURE 3** Gene expression analysis. Parental MeT-5A cells and each cell clone were seeded in a 6-well plate and incubated for 24 hours. Total RNA was extracted and cDNA microarray analysis was carried out using an Agilent Whole Human Genome cDNA Microarray Kit (4 × 44K; design ID, 026652; Agilent Technologies, Santa Clara, CA, USA). A, Heatmap of upregulated genes (17 genes; fold change, >5.0) and downregulated genes (77 genes, fold change <0.2) in neurofibromatosis type 2 knockout (NF2-KO) cell clones (#1 and #2), compared with NF2-WT cell clones (#1 and #2) and parental (P) cells. The heatmap was constructed using normalized values of each sample with TreeView (Cluster 3.0) software (<http://jtreeview.sourceforge.net>). Corresponding upregulated or downregulated genes in the heatmap are shown at the right side. B, RT-PCR analysis of mRNA expression levels of the upregulated or downregulated genes in the MeT-5A cell clones. Representative results of agarose gel electrophoresis of RT-PCR products from parental MeT-5A cells, control NF2-WT cell clones (#1 and #2), NF2-KO cell clones (#1 and #2), and NF2-KO cell clones exogenously expressing NF2 (NF2/NF2-KO #1 and #2) are shown

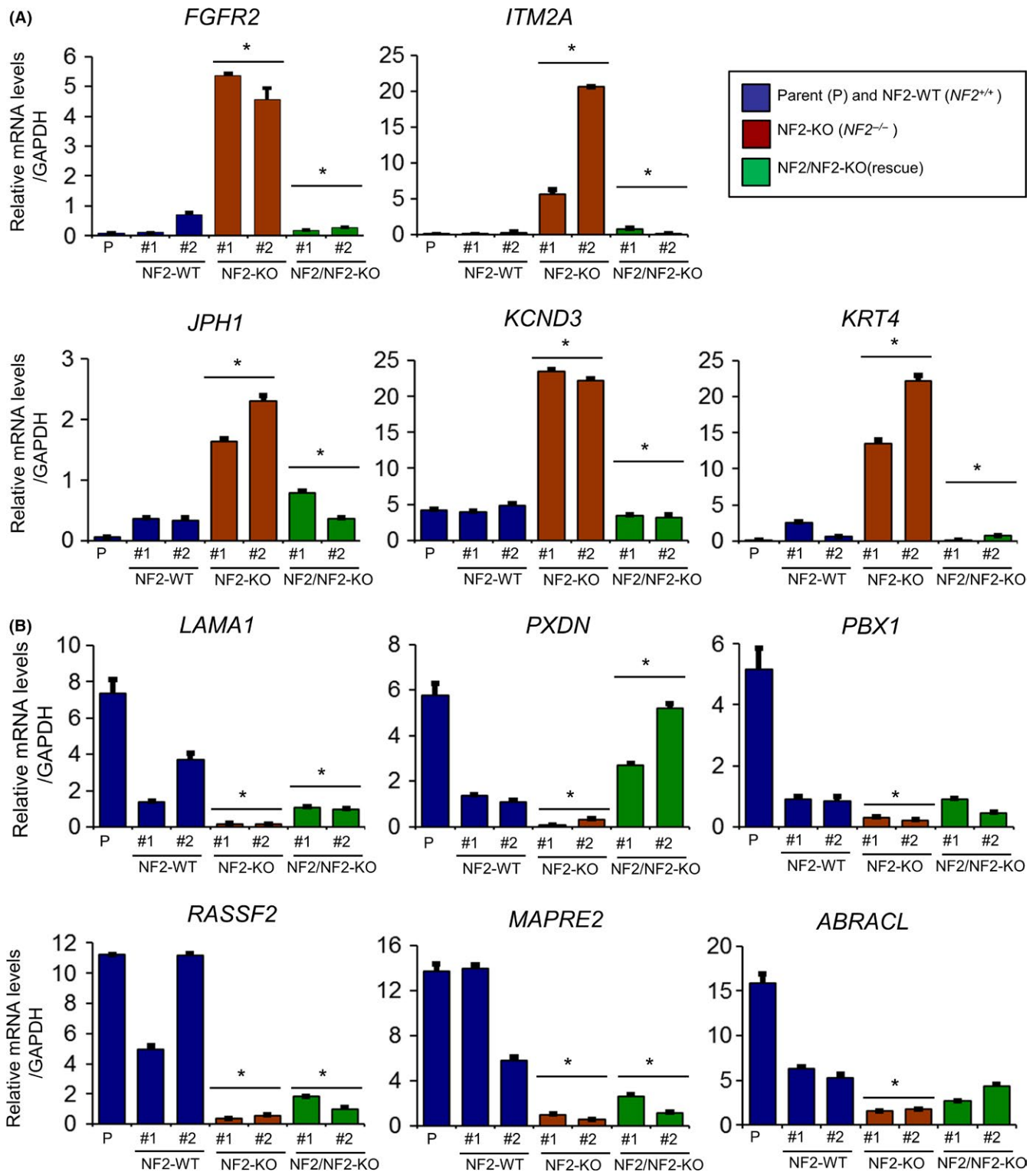


**FIGURE 4** Quantitative real-time PCR analysis. Eleven genes, whose upregulation (A) or downregulation (B) in neurofibromatosis type 2 knockout (NF2-KO) cell clones was detected in cDNA microarray analysis, were subjected to quantitative real-time PCR analysis using the SYBR Green method. Relative gene expression levels are shown after normalization to *GAPDH* mRNA expression. Mean values were compared with the normal control value to calculate relative amounts of transcripts. Data are presented as mean  $\pm$  SEM ( $n = 3$ ). \*Statistically significant difference ( $P < .05$ )

parental cells, NF2-WT, and NF2-KO clones. To compare the gene expression profiles of NF2-KO with NF2-WT and parental cells, normalized values of raw microarray data were calculated and clustered

according to the differential gene expression. We successively detected 17 genes whose expression was upregulated more than 5-fold (Table S3) and 77 genes whose expression was downregulated

less than 0.2-fold (Table S4). In addition, with the aid of Gene Set Enrichment Analysis, the genes related to positive regulation of the cell cycle were shown to be significantly activated in the NF2-KO clones compared with the levels in the NF2-WT clones (Figure S1A). The results of Gene Set Enrichment Analysis also showed that some of the downregulated genes overlapped with the genes whose expression levels were reported to be lower in patients with biphasic-type MPM than in those with epithelial-type MPM (Figure S1B).<sup>26</sup> In addition, the clustering of the 94 genes showed a distinct gene expression pattern between NF2-KO and NF2-WT and parental cells (Figure 3A). To further confirm the effect of NF2 on the gene expression changes in the NF2-KO clone, we undertook RT-PCR analyses for the 18 candidate genes related to cell survival, proliferation, or tumorigenesis. Agarose gel electrophoresis of RT-PCR products

showed decreases in the mRNA expression of *LAMA1*, *JAG1*, *NKD2*, *PBX1*, *RASSF2*, *PXDN*, *ABRACL*, *ACTA2*, *COLEC12*, *MGST2*, *PLAU*, *MAPRE2*, and *IFI27* genes, and increases in the expression of *FGFR2*, *KCND3*, *KRT4*, *MET*, *FAM155A*, and *ITM2A* in the NF2-KO clones, compared with the levels in NF2-WT and parental cells (Figure 3B). We found that the changes in mRNA expression were all abrogated in the NF2/NF2-KO clones except the *MGST2*, *COLEC12*, *NKD2*, *ACTA2*, *IFI27*, and *FAM155A* genes (Figure 3B). We undertook further qRT-PCR to precisely compare the gene expression levels among the clones. The results showed that the mRNA expression of *FGFR2*, *ITM2A*, *JPH1*, *KCND3*, and *KRT4* significantly increased, whereas that of *LAMA*, *PXDN*, *PBX1*, *RASSF2*, *MAPE2*, and *ABRACL* significantly decreased in the NF2-KO cells (Figure 4). Similarly, the changes in gene expression were abrogated in the exogenous NF2/NF2-KO clones

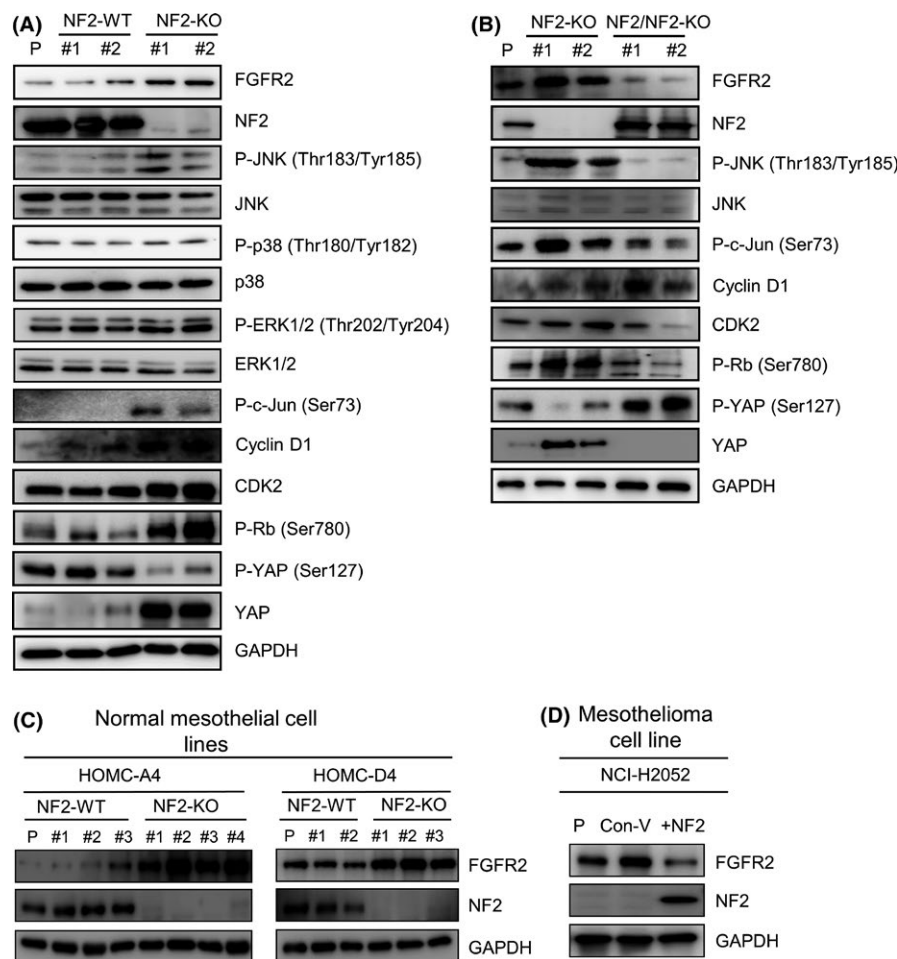


**FIGURE 5** Protein expression analyses. A, Western blot analysis showing protein expression of neurofibromatosis type 2 (NF2), fibroblast growth factor receptor 2 (FGFR2), phosphorylation levels of MAPKs (P-ERK1/2, P-JNK, and P-p38), phospho-c-Jun (P-c-Jun), phospho-retinoblastoma (P-Rb), cyclin-dependent kinase 2 (CDK2), Cyclin D1, and phospho-yes-associated protein (P-YAP) in the parental MeT-5A cells, control NF2-WT clones, and NF2-KO clones. Cell lysates obtained were subjected to western blotting analysis to detect each protein level by using specific Abs. B, Effect of exogenous NF2 expression in NF2/NF2-KO clones on the protein levels of FGFR2, P-JNK, P-c-Jun, cyclin D1, CDK2, P-Rb, and P-YAP. The NF2/pcDNA3.1 vector was transfected in the NF2-KO clones using a 4D-Nucleofector instrument (Lonza Japan, Tokyo, Japan). C, Western blot analysis showing the protein expression of NF2 and FGFR2 in NF2-knockout human mesothelial cell lines HOMC-A4 and HOMC-D4. D, Western blot analysis showing the protein expression of NF2 and FGFR2 due to overexpression of NF2 in the mesothelioma cell line NCI-H2052. Cells were transfected with control pcDNA3.1 (Con-V) and WT NF2/pcDNA3.1 vectors. After transfection, the cells were incubated for 48 hours, washed with PBS and lysed in loading buffer. The cell lysates obtained were subjected to western blotting analysis. GAPDH was used as an internal control

(Figure 4). The results of qRT-PCR further confirmed that rescuing NF2 had no significant effect on the mRNA expression of *MGST2*, *COLEC12*, *NKD2*, *ACTA2*, *IFI27*, or *FAM155A* genes (Figure S2). These results strongly suggest that the affected gene products might function downstream of NF2 signaling.

### 3.3 | Effect of NF2 knockout on FGFR2 expression and cell cycle-related molecules

As therapy targeting the FGF-FGFR axis has emerged as a novel anticancer application in a panel of solid cancers,<sup>27-29</sup> we next focused on FGFR2, whose expression was found to increase in the NF2-KO MeT-5A cells (Figure 5A). In addition, the phosphorylation levels of both ERK and JNK MAPKs, increased in the NF2-KO clones, whereas the level of p38 MAPK remained constant (Figure 5A). Similarly, the phosphorylation level of c-Jun increased in the NF2-KO cell clones (Figure 5A). Furthermore, both phosphorylation levels of a cell cycle regulator, Rb, and protein expression levels of CDK2 and cyclin D1 increased in the NF2-KO cell clones (Figure 5A). We also observed that, in spite of an abundant increase in the total YAP level, the YAP phosphorylation level decreased in the NF2-KO cell clones (Figure 5A). To confirm the effect of NF2 on the expression of

these proteins, we utilized the exogenous NF2/NF2-KO cell clones. Rescuing of NF2 protein expression resulted in a reduction in FGFR2 expression in the NF2/NF2-KO clones compared with that in the NF2-KO clones (Figure 5B), consistent with the results of qRT-PCR analysis. Furthermore, the other changes in protein expression and phosphorylation were all abrogated in the exogenous NF2/NF2-KO cell clones (Figure 5B). Additionally, knockout of NF2 in other normal mesothelial cell lines, HOMC-A4, and HOMC-D4 substantially increased the FGFR2 protein levels (Figure 5C). In another human mesothelioma cell line NCI-H2052, we did not find any endogenous expression of NF2 protein. Interestingly, exogenous expression of NF2 in this cell line clearly decreased the FGFR2 protein level (Figure 5D). These results suggest that FGFR2 expression might be negatively regulated by NF2 signaling in the mesothelial cells.

### 3.4 | Knockout of FGFR2 gene retards cell proliferation in the absence of NF2 gene

To clarify the role of FGFR2 in the proliferation of NF2-KO cells, we generated NF2 and FGFR2 double knockout cell clones (hereafter called NF2/FGFR2-DKO #1 and #2) as well as FGFR2 knockout cell clone (hereafter called FGFR2-KO). The MTT assay showed that the

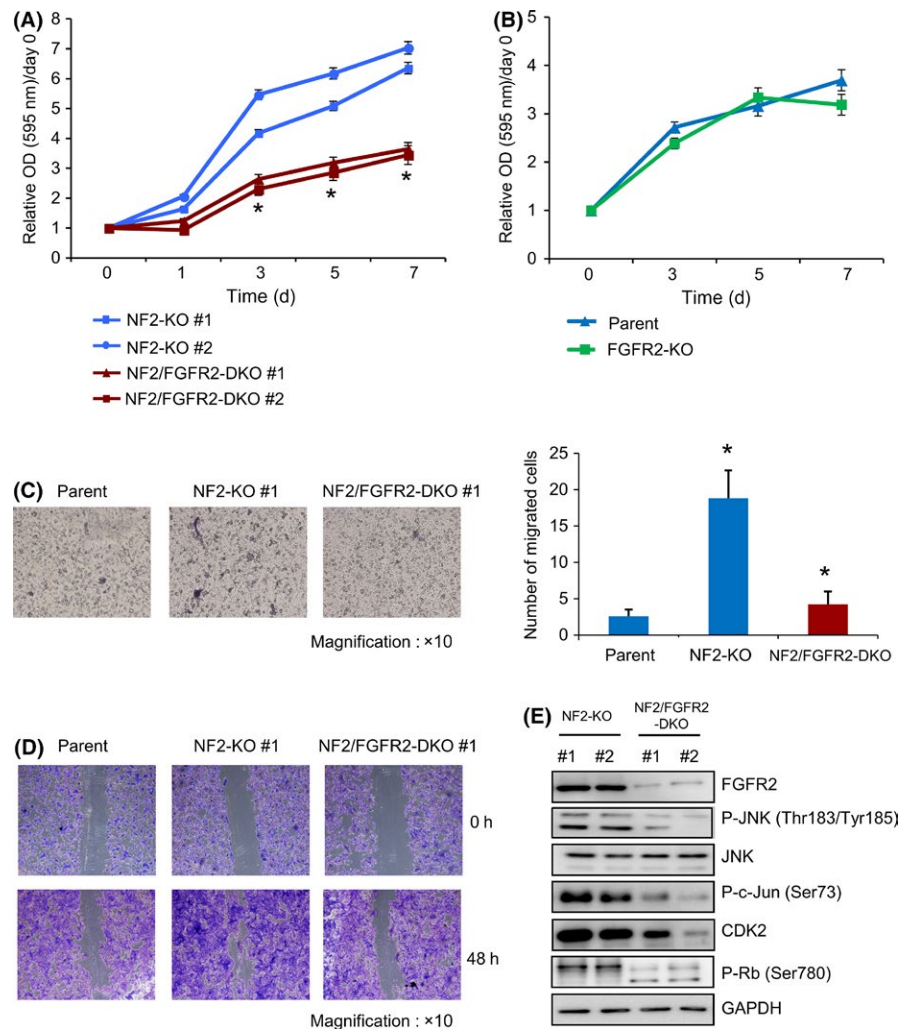


**FIGURE 6** Cellular phenotype of neurofibromatosis type 2/fibroblast growth factor receptor 2 (NF2/FGFR2) double knockout (DKO) in MeT-5A cells. A, MTT analysis of the growth rate of NF2-KO cell clones (#1 and #2) and NF2/FGFR2-DKO cell clones (#1 and #2) in MeT-5A cells. The optical density (OD; 595 nm) at each time point (days 0, 3, 5, and 7) is presented as the mean  $\pm$  SEM (n = 6). Data of growth ratio are expressed relative to the optical densities detected at day 0, which are arbitrarily defined as 1. B, Representative MTT assay for the growth ratio of parental and FGFR2-KO cell clone. C, D, Representative images of Boyden chamber migration assay (C) and scratch assay (D). E, Western blotting showing the protein expression of FGFR2, P-JNK, JNK, P-c-Jun, cyclin-dependent kinase 2 (CDK2), phospho-retinoblastoma (P-Rb), and GAPDH in NF2-KO cells and NF2/FGFR2-DKO cells. \*Statistically significant difference ( $P < .05$ )



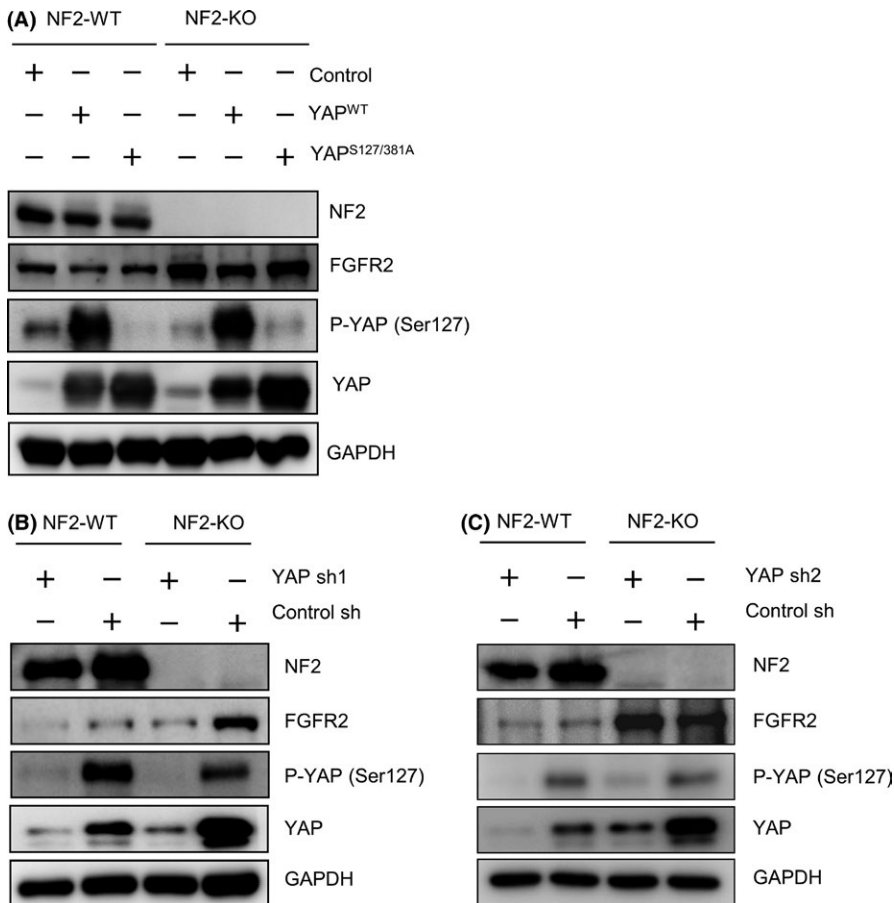


**FIGURE 7** Effect of yes-associated protein (YAP) expression and YAP knockdown on fibroblast growth factor receptor 2 (FGFR2) expression. A, Effect of exogenous expression of YAP on FGFR2 expression. Neurofibromatosis type 2 (NF2)-WT and knockout (NF2-KO) cells were transfected with control pcDNA3.1, WT YAP/pcDNA3.1, or active mutant YAP<sup>S127/381A</sup>/pcDNA3.1 by using nucleofection. After 48 hours of incubation, the cell lysates were prepared and subjected to western blot analysis. Each protein was detected using specific Abs, and representative images are shown. B,C, Effect of YAP knockdown on FGFR2 expression. NF2-WT and NF2-KO cells were transfected with either YAP sh1 (B) or YAP sh2 (C) and control shRNA vectors. After 48 hours of incubation, the cell lysates were prepared and subjected to western blot analysis, as described above

cell growth ratio significantly decreased in the NF2/FGFR2-DKO clones compared with that in the NF2-KO clones (Figure 6A). In contrast, the growth ratio did not significantly alter between FGFR2-KO and parental cells (Figure 6B). In addition, disruption of *FGFR2* in NF2-KO cells suppressed the *NF2* knockout-induced migration and wound healing activities of NF2/FGFR2-DKO cells (Figures 6C,D). Furthermore, western blot analysis showed that the phosphorylation levels of JNK and c-Jun were downregulated in the NF2/FGFR2-DKO clones (Figure 6E). We also found that the protein level of CDK2 and the phosphorylation level of Rb decreased in the NF2/FGFR2-DKO clones (Figure 6E). These results indicate the possibility that FGFR2 could play important role in the proliferation of mesothelioma cells with *NF2* mutation.

### 3.5 | Relationship between YAP activity and FGFR2 expression

It has been reported that *NF2* mutation activates a downstream YAP oncogenic signaling pathway, which leads to cell cycle progression and induces carcinogenesis.<sup>30</sup> Consistent with a previous study reporting the decreased level of YAP phosphorylation in *NF2*-deficient cells,<sup>31</sup> we also observed the decreased phosphorylation level of YAP in our NF2-KO clones (Figure 5A). To clarify the involvement of YAP in FGFR2 expression, we examined the effects of exogenous YAP expression and/or knockdown of YAP on FGFR2 expression.

The FGFR2 protein expression was not upregulated by exogenous expression of either constitutively active YAP<sup>S127/381A</sup> mutant or WT YAP, regardless of *NF2* loss (Figure 7A). Consequently, *NF2* knockout-induced FGFR2 expression did not significantly change under YAP knockdown with YAP sh2 vector, whereas it decreased under YAP knockdown with YAP sh1 vector (Figures 7B,C). We also found that the phosphorylation level of c-Jun increased after exogenous YAP expression, whereas it decreased following YAP knockdown (Figure S3).

### 3.6 | Immunohistochemistry for FGFR2 expression in patients with MPM

Finally, we undertook immunohistochemical analyses to examine the protein expression level of FGFR2 in 23 malignant mesotheliomas and 10 normal mesothelium tissue samples (Table 1, Figure 8A). Microscopy analysis showed 3 strong (3+), 8 moderate (2+), and 2 weak (1+) FGFR2-positive signals in MPM tissues, whereas only 1 weak (1+) signal of FGFR2 expression was found in normal mesothelium tissues (Table 1, Figure 8B). Interestingly, the rate of positivity for FGFR2 signals in the NF2-negative MPM tissues (11 of 12 tissues, 91.7%) was significantly higher than that in the NF2-positive MPM tissues (2 of 11 tissues, 18.2%; Figure 8). Our analysis using data in the public domain (GSE2549 and GSE29354, deposited in GEO datasets) clarified that *FGFR2* mRNA expression in patients with MPM was higher than that

**TABLE 1** Summary of immunohistochemistry in this study

Case	Sex	Age, years	Organ	Pathology	Stage	Type	NF2 intensity	FGFR2 intensity
1	F	70	Abdominal cavity	Epithelial malignant mesothelioma	IV	Malignant	2+	2+
2	M	60	Abdominal cavity	Malignant mesothelioma of abdominal membrane	II	Malignant	3+	0
3	M	5	Abdominal cavity	Malignant mesothelioma	N/A	Malignant	0	2+
4	M	60	Abdominal cavity	Malignant mesothelioma of abdominal membrane	N/A	Malignant	2+	0
5	F	47	Abdominal cavity	Malignant mesothelioma (sparse)	I	Malignant	0	2+
6	M	33	Abdominal cavity	Epithelial malignant mesothelioma of abdominal membrane	IV	Malignant	2+	0
7	F	38	Abdominal cavity	Malignant mesothelioma	IV	Malignant	0	2+
8	M	63	Retropertoneum	Malignant mesothelioma	N/A	Malignant	3+	2+
9	M	48	Heart	Epithelial malignant mesothelioma of abdominal membrane	II	Malignant	2+	0
10	M	43	Heart	Epithelial malignant mesothelioma	IIIB	Malignant	0	2+
11	F	23	Lung	Malignant mesothelioma	II	Malignant	0	1+
12	F	18	Lung	Malignant mesothelioma	I	Malignant	0	1+
13	F	56	Mediastinum	Malignant mesothelioma of pleura	II	Malignant	2+	0
14	F	58	Pleura	Malignant mesothelioma (sparse)	I	Malignant	2+	0
15	F	22	Pleura	Malignant mesothelioma of thoracic cavity	I	Malignant	0	2+
16	F	70	Pleura	Malignant mesothelioma of right pleura	II	Malignant	0	3+
17	M	47	Pleura	Malignant mesothelioma of left pleura	II	Malignant	0	0
18	M	49	Pleura	Malignant mesothelioma	I	Malignant	0	3+
19	F	64	Pleura	Epithelial malignant mesothelioma of chest wall	II	Malignant	0	3+

(Continues)

TABLE 1 (Continued)

Case	Sex	Age, years	Organ	Pathology	Stage	Type	NF2 intensity	FGFR2 intensity
20	M	49	Pleura	Malignant mesothelioma	I	Malignant	0	2+
21	M	83	Pleura	Malignant mesothelioma	III	Malignant	2+	0
22	M	50	Cardiac pericardium	Malignant mesothelioma	I	Malignant	2+	0
23	M	43	Cardiac pericardium	Malignant mesothelioma	I	Malignant	3+	0
24	M	34	Pleura	Normal mesothelium tissue (lung tissue)	N/A	Normal	2+	0
25	F	15	Cardiac pericardium	Normal mesothelium tissue	N/A	Normal	3+	0
26	M	28	Cardiac pericardium	Normal mesothelium tissue (sparse)	N/A	Normal	2+	0
27	F	27	Cardiac pericardium	Normal mesothelium tissue	N/A	Normal	2+	0
28	M	43	Cardiac pericardium	Normal mesothelium tissue	N/A	Normal	3+	0
29	M	19	Cardiac pericardium	Normal mesothelium tissue	N/A	Normal	2+	0
30	F	21	Lung	Normal mesothelium tissue	N/A	Normal	3+	0
31	F	21	Lung	Normal mesothelium tissue (lung tissue)	N/A	Normal	3+	1+
32	M	47	Lung	Normal mesothelium tissue	N/A	Normal	2+	0
33	M	19	Lung	Normal mesothelium tissue (sparse)	N/A	Normal	3+	0

Intensity of the positive signals for neurofibromatosis type 2 (NF2) and fibroblast growth factor receptor 2 (FGFR2) was evaluated by 2 investigators. F, female; M, male; N/A, not analyzed.

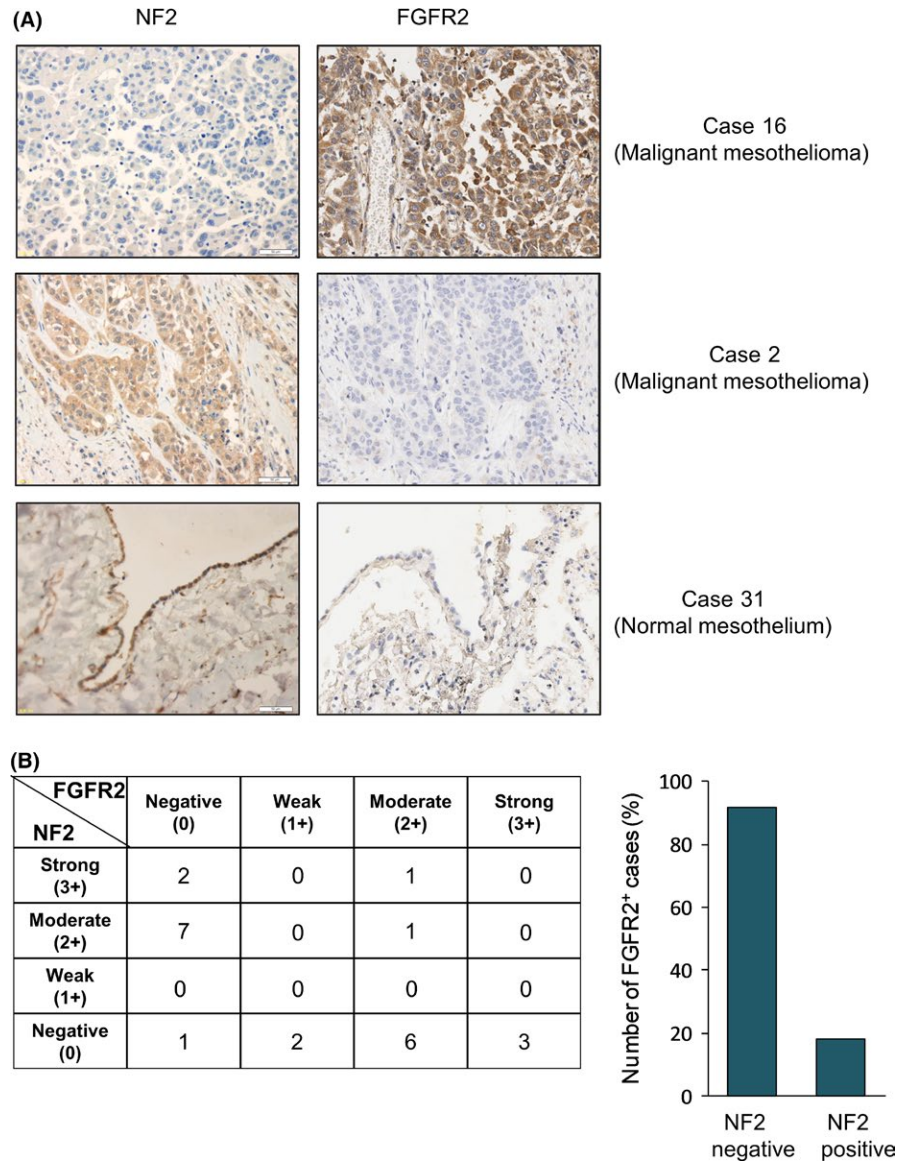


**FIGURE 8** Immunohistochemistry (IHC) for neurofibromatosis type 2 (NF2) and fibroblast growth factor receptor 2 (FGFR2) expression. A, Representative results of IHC for NF2 (left panels) and FGFR2 (right panels) expression in NF2-negative malignant pleural mesothelioma (MPM) tissue (upper panels, case 16), NF2-positive MPM tissue (middle panels, case 2), and normal mesothelium tissue (lower panels, case 31). B, Summary of IHC results in MPM tissues. The immunoreactivities were independently evaluated by 2 investigators. The intensity of staining was scored as strong (3+), moderate (2+), weak (1+), or negative (0). The bar graph represents the percentage of total number of cases with FGFR2 expression (strong, moderate and weak) in the MPM tissues with NF2 negative or NF2 positive (strong, moderate, and weak) cases.

in normal pleura (Figure S4A). Notably, overall survival in the MPM patients with high FGFR2 expression was shorter than in those with low FGFR2 expression in both datasets (Figure S4B). Collectively, these results strongly indicate the possibility that the loss of *NF2* results in the increased expression of FGFR2, which might be closely associated with poor prognosis in MPM.

## 4 | DISCUSSION

Recent molecular biological studies have revealed frequent genetic alterations of 3 key tumor suppressor genes, *NF2*, *CDKN2A*, and *BAP1*, in MPM. In this study, we generated *NF2* knockout isogenic cell clones using a human immortalized normal mesothelial cell line, MeT-5A, and showed that the loss of *NF2* enhances cell proliferation with global gene expression changes. Our study strongly suggests that FGFR2 expression might be the downstream event of *NF2* in MPM tissues and be correlated with overall survival of MPM

patients. Furthermore, we showed that the loss of *FGFR2* attenuates the proliferation of *NF2*-KO MeT-5A cells.

The CRISPR/Cas9 system makes it readily possible to disrupt target genes by inducing insertion/deletion and to introduce specific gene polymorphism/mutation by inducing homologous recombination. Our cellular model presented here is the first to reveal the gene expression profile under complete disruption of *NF2* in human normal mesothelial cells. Using the *NF2*-KO cell clones, we found that loss of the *NF2* gene in MeT-5A cells enhances cell proliferation, clonogenicity, and cell migration, as previously described.<sup>19</sup> Using comprehensive gene expression analysis, we found that gene expression in the *NF2*-KO cell clones was distinct from that in the *NF2*-WT cells. Quantitative RT-PCR analysis revealed that the mRNA expression of *FGFR2*, *ITAM2A*, *JPH1*, *KCND3*, *KRT4*, *LAMA1*, *PXDND*, *PBX1*, and *RASSF2* was closely associated with *NF2* expression. Our results of gene expression profiling showed that the loss of *NF2* significantly enhanced the expression of genes related to positive regulation of the cell cycle phase and suppressed the expression of certain other

genes, some of which were reported to be downregulated in malignant mesothelioma.<sup>26</sup>

Fibroblast growth factor receptor family protein has been shown to be amplified and overexpressed in several cancer types.<sup>32-37</sup> Expression of FGFR2 protein was observed in several types of cancer including breast and gastric cancer.<sup>38,39</sup> Fibroblast growth factor receptor 1 has been reported to be a growth driver in MPM.<sup>28,40</sup> Recent data reported by The Cancer Genome Atlas lung squamous cell carcinoma project showed that the FGFR tyrosine kinases are some of the most frequently altered kinase families in lung squamous cell carcinoma.<sup>41</sup> Interestingly, Quispel-Janssen et al<sup>29</sup> recently reported that a subgroup of immortalized and primary MPM lines appeared to be highly sensitive to FGFR inhibition. They also showed an association between *BAP1* loss and increased expression of the receptors FGFR1/3 and ligands FGF9/18.<sup>29</sup> Taken together with these reports, our study indicates the possibility that the FGF-FGFR axis could play an important role in the molecular pathogenesis of MPM.

Our immunohistochemical study showed that FGFR2 was commonly expressed (in 11 of 12) in NF2-negative MPM tissues, whereas it was rarely expressed (in 2 of 11) in NF2-positive MPM tissues. Additionally, *NF2* loss resulted in the increased expression of *FGFR2*, and subsequent rescue of *NF2* expression decreased its expression in MeT-5A cells. In other normal mesothelial cell lines HOMC-A4 and HOMC-D4, we also found that knockout of *NF2* causes a substantial increase in FGFR2 protein level. In contrast, exogenous expression of *NF2* in an NF2-deficient human mesothelioma cell line NCI-H2052 led to a decrease in FGFR2 protein level. These results indicate the possibility that FGFR2 expression is intimately regulated by *NF2* expression. Furthermore, knockout of *FGFR2* in NF2-KO cells led to retardation of cell growth, accompanied by decreases in the phosphorylation of JNK, c-Jun, and Rb, as well as the expression of CDK2. These results strongly suggest that FGFR2 could play a pivotal role in the proliferation of NF2-KO cells.

A transcription factor in the downstream of *NF2* signaling, YAP/TAZ, was reported to be critical for the carcinogenesis of mesothelial cells with *NF2* loss.<sup>30,31</sup> Our previous study reported c-Jun amplification in a panel of MPM tumors.<sup>42</sup> In this study, we observed that overexpression of constitutively active YAP mutant does not alter the FGFR2 protein level in the NF2-KO clone, whereas it increases the phosphorylation levels of c-Jun and cyclin D1. In addition, we found that FGFR2 protein expression does not significantly change under YAP knockdown with YAP sh2 vector, whereas it decreases under YAP knockdown with YAP sh1 vector in the NF2-KO clone. Our data could not exclude the possibility that YAP activity is related to *NF2* knockout-induced FGFR2 expression. Further studies are necessary to clarify the molecular mechanism by which loss of *NF2* increases *FGFR2* expression in mesothelial cells.

In conclusion, this study is the first to show the global gene expression changes following *NF2* loss in a human mesothelial cell line, MeT-5A. The CRISPR/Cas9-mediated loss of *NF2* enhanced the

proliferation of cells and the expression of *FGFR2*, the subsequent disruption of which significantly suppressed the phosphorylation of cell cycle-related molecules as well as enhanced the proliferation of the cells. Although the molecular mechanism underlying *NF2* loss-mediated upregulation of *FGFR2* remains unclear, it was found that *FGFR2* expression was inversely correlated with *NF2* expression in MPM tissues and was associated with the survival of MPM patients. Our study strongly suggests that FGFR2 signaling might play a pivotal role in the proliferation of MPM cells. Further studies are warranted to understand the role of FGFR2 in the molecular pathogenesis in *NF2*-disrupted MPM cells. Our findings could help to clarify the importance of the FGFR signaling pathway in MPM and to develop specific molecular-targeted drugs for the treatment of patients with MPM.

## ACKNOWLEDGEMENT

We thank Dr. Y. Sekido, Division of Molecular Oncology, Aichi Cancer Center Research Institute for providing the cell lines. This work was partly supported by a Hirose International Scholarship Foundation research grant.

## CONFLICT OF INTEREST

There are no known conflicts of interest associated with this publication.

## ORCID

Sivasundaram Karnan  <http://orcid.org/0000-0003-2165-7565>

Akinobu Ota  <http://orcid.org/0000-0002-6296-2921>

## REFERENCES

1. Pass HI, Vogelzang N, Hahn S, Carbone M. Malignant pleural mesothelioma. *Curr Probl Cancer*. 2004;28:93-174.
2. Bolognesi C, Martini F, Tognon M, et al. A molecular epidemiology case control study on pleural malignant mesothelioma. *Cancer Epidemiol Biomarkers Prev*. 2005;14:1741-1746.
3. Patel SC, Dowell JE. Modern management of malignant pleural mesothelioma. *Lung Cancer*. 2016;7:63-72.
4. Vogelzang NJ, Rusthoven JJ, Symanowski J, et al. Phase III study of pemetrexed in combination with cisplatin versus cisplatin alone in patients with malignant pleural mesothelioma. *J Clin Oncol*. 2003;21:2636-2644.
5. Fung H, Kow YW, Van Houten B, Mossman BT. Patterns of 8-hydroxydeoxyguanosine formation in DNA and indications of oxidative stress in rat and human pleural mesothelial cells after exposure to crocidolite asbestos. *Carcinogenesis*. 1997;18:825-832.
6. Sekido Y. Molecular pathogenesis of malignant mesothelioma. *Carcinogenesis*. 2013;34:1413-1419.
7. Bott M, Brevet M, Taylor BS, et al. The nuclear deubiquitinase BAP1 is commonly inactivated by somatic mutations and 3p21.1 losses in malignant pleural mesothelioma. *Nat Genet*. 2011;43:668-672.
8. Guo G, Chmielecki J, Goparaju C, et al. Whole-exome sequencing reveals frequent genetic alterations in BAP1, NF2, CDKN2A,

- and CUL1 in malignant pleural mesothelioma. *Cancer Res.* 2015;75:264-269.
9. Cheng JQ, Jhanwar SC, Klein WM, et al. p16 alterations and deletion mapping of 9p21-p22 in malignant mesothelioma. *Cancer Res.* 1994;54:5547-5551.
  10. Thurneysen C, Opitz I, Kurtz S, Weder W, Stahel RA, Felley-Bosco E. Functional inactivation of NF2/merlin in human mesothelioma. *Lung Cancer.* 2009;64:140-147.
  11. Bianchi AB, Mitsunaga SI, Cheng JQ, et al. High frequency of inactivating mutations in the neurofibromatosis type 2 gene (NF2) in primary malignant mesotheliomas. *Proc Natl Acad Sci USA.* 1995;92:10854-10858.
  12. Sheffield BS, Hwang HC, Lee AF, et al. BAP1 Immunohistochemistry and p16 FISH to separate benign from malignant mesothelial proliferations. *Am J Surg Pathol.* 2015;39:977-982.
  13. Farzin M, Toon CW, Clarkson A, et al. Loss of expression of BAP1 predicts longer survival in mesothelioma. *Pathology.* 2015;47:302-307.
  14. Dacic S, Kothmaier H, Land S, et al. Prognostic significance of p16/cdkn2a loss in pleural malignant mesotheliomas. *Virchows Arch.* 2008;453:627-635.
  15. Kobayashi N, Toyooka S, Yanai H, et al. Frequent p16 inactivation by homozygous deletion or methylation is associated with a poor prognosis in Japanese patients with pleural mesothelioma. *Lung Cancer.* 2008;62:120-125.
  16. López-Ríos F, Chuaí S, Flores R, et al. Global gene expression profiling of pleural mesotheliomas: overexpression of aurora kinases and P16/CDKN2A deletion as prognostic factors and critical evaluation of microarray-based prognostic prediction. *Cancer Res.* 2006;66:2970-2979.
  17. Xiao GH, Gallagher R, Shetler J, et al. The NF2 tumor suppressor gene product, merlin, inhibits cell proliferation and cell cycle progression by repressing cyclin D1 expression. *Mol Cell Biol.* 2005;25:2384-2394.
  18. Fleury-Feith J, Lecomte C, Renier A, et al. Hemizyosity of Nf2 is associated with increased susceptibility to asbestos-induced peritoneal tumours. *Oncogene.* 2003;22:3799-3805.
  19. Kakiuchi T, Takahara T, Kasugai Y, et al. Modeling mesothelioma utilizing human mesothelial cells reveals involvement of phospholipase-C beta 4 in YAP-active mesothelioma cell proliferation. *Carcinogenesis.* 2016;37:1098-1109.
  20. Ran FA, Hsu PD, Wright J, Agarwala V, Scott DA, Zhang F. Genome engineering using the CRISPR-Cas9 system. *Nat Protoc.* 2013;8:2281-2308.
  21. Yamaji M, Ota A, Wahiduzzaman M, et al. Novel ATP-competitive Akt inhibitor afuresertib suppresses the proliferation of malignant pleural mesothelioma cells. *Cancer Med.* 2017;6:2646-2659.
  22. Wahiduzzaman M, Ota A, Karnan S, et al. Novel combined Ato-C treatment synergistically suppresses proliferation of Bcr-Abl-positive leukemic cells in vitro and in vivo. *Cancer Lett.* 2018;433:117-130.
  23. Ito T, Matsubara D, Tanaka I, et al. Loss of YAP1 defines neuroendocrine differentiation of lung tumors. *Cancer Sci.* 2016;107:1527-1538.
  24. Tranchant R, Quétel L, Tallet A, et al. Co-occurring mutations of tumor suppressor genes, LATS2 and NF2, in malignant pleural mesothelioma. *Clin Cancer Res.* 2017;23:3191-3202.
  25. Bueno R, Stawiski EW, Goldstein LD, et al. Comprehensive genomic analysis of malignant pleural mesothelioma identifies recurrent mutations, gene fusions and splicing alterations. *Nat Genet.* 2016;48:407-416.
  26. Borczuk AC, Cappellini GC, Kim HK, Hesdorffer M, Taub RN, Powell CA. Molecular profiling of malignant peritoneal mesothelioma identifies the ubiquitin-proteasome pathway as a therapeutic target in poor prognosis tumors. *Oncogene.* 2007;26:610-617.
  27. Chae YK, Ranganath K, Hammerman PS, et al. Inhibition of the fibroblast growth factor receptor (FGFR) pathway: the current landscape and barriers to clinical application. *Oncotarget.* 2017;8:16052-16074.
  28. Marek LA, Hinz TK, von Mässenhausen A, et al. Non-amplified FGFR1 is a growth driver in malignant pleural mesothelioma. *Mol Cancer Res.* 2014;12:1460-1469.
  29. Quispel-Janssen JM, Badhai J, Schunselaar L, et al. Comprehensive pharmacogenomic profiling of malignant pleural mesothelioma identifies a subgroup sensitive to FGFR inhibition. *Clin Cancer Res.* 2018;24:84-94.
  30. Felley-Bosco E, Stahel R. Hippo/YAP pathway for targeted therapy. *Transl Lung Cancer Res.* 2014;3:75-83.
  31. Zhang N, Bai H, David KK, et al. The Merlin/NF2 tumor suppressor functions through the YAP oncoprotein to regulate tissue homeostasis in mammals. *Dev Cell.* 2010;19:27-38.
  32. Katoh Y, Katoh M. FGFR2-related pathogenesis and FGFR2-targeted therapeutics. *Int J Mol Med.* 2009;23:307-311.
  33. Grose R, Dickson C. Fibroblast growth factor signaling in tumorigenesis. *Cytokine Growth Factor Rev.* 2005;16:179-186.
  34. Moffa AB, Tannheimer SL, Ethier SP. Transforming potential of alternatively spliced variants of fibroblast growth factor receptor 2 in human mammary epithelial cells. *Mol Cancer Res.* 2004;2:643-652.
  35. Toyokawa T, Yashiro M, Hirakawa K. Co-expression of keratinocyte growth factor and K-sam is an independent prognostic factor in gastric carcinoma. *Oncol Rep.* 2009;21:875-880.
  36. Cha Y, Kim HP, Lim Y, Han SW, Song SH, Kim TY. FGFR2 amplification is predictive of sensitivity to regorafenib in gastric and colorectal cancers in vitro. *Mol Oncol.* 2018;12:993-1003. <https://doi.org/10.1002/1878-0261.12194>.
  37. Marshall ME, Hinz TK, Kono SA, et al. Fibroblast growth factor receptors are components of autocrine signaling networks in head and neck squamous cell carcinoma cells. *Clin Cancer Res.* 2011;17:5016-5025.
  38. Fletcher MN, Castro MA, Wang X, et al. Master regulators of FGFR2 signalling and breast cancer risk. *Nat Commun.* 2013;4:2464.
  39. Su X, Zhan P, Gavine PR, et al. FGFR2 amplification has prognostic significance in gastric cancer: results from a large international multicentre study. *Br J Cancer.* 2014;110:967-975.
  40. Weiss J, Sos ML, Seidel D, et al. Frequent and focal FGFR1 amplification associates with therapeutically tractable FGFR1 dependency in squamous cell lung cancer. *Sci Transl Med.* 2010;2:62ra93.
  41. Hammerman PS, Lawrence MS, Voet D, et al. Comprehensive genomic characterization of squamous cell lung cancers. *Nature.* 2012;489:519-525.
  42. Taniguchi T, Karnan S, Fukui T, et al. Genomic profiling of malignant pleural mesothelioma with array-based comparative genomic hybridization shows frequent non-random chromosomal alteration regions including JUN amplification on 1p32. *Cancer Sci.* 2007;98:438-446.

## SUPPORTING INFORMATION

Additional supporting information may be found online in the Supporting Information section at the end of the article.

**How to cite this article:** Wahiduzzaman M, Karnan S, Ota A, et al. Establishment and characterization of CRISPR/Cas9-mediated *NF2*<sup>-/-</sup> human mesothelial cell line: Molecular insight into fibroblast growth factor receptor 2 in malignant pleural mesothelioma. *Cancer Sci.* 2019;110:180-193. <https://doi.org/10.1111/cas.13871>